Triple Junctions and Low Angle Boundaries

By

Vinay Rodrigues
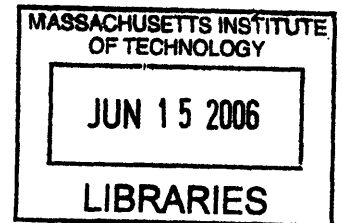
SUBMITTED TO THE DEPARTMENT OF MATERIALS SCIENCE AND
ENGINEERING IN PARTIALL THE FUFILLMENT OF THE REQUIREMENTS FOR
THE DEGREE OF

BACHELOR OF SCIENCE IN MATERIALS SCIENCE AND ENGINEERING
AT THE
MASSACHUSETTS INSTITUTE OF TECHNOLOGY

JUNE 2006

Signature of Author: _____
Department of Materials Science and Engineering
May 31, 2006

Certified by:_____
Christopher A. Schuh
Danae and Vasilios Associate Professor of Metallurgy
Thesis Supervisor

Accepted by:_____
Caroline A. Ross, Ph.D.
Professor of Materials Science and Engineering
Chair, Departmental Undergraduate Committee

Triple junctions and low angle boundaries

By

Vinay Rodrigues

Abstract
Certain properties, such as cracking or corrosion, can occur mainly along grain boundaries. Certain types of boundaries may be more beneficial for material properties. The way that the boundaries are connected in a material can determine how boundaries will affect properties, for instance, whether or not crack resistant boundaries will arrest the growth of a crack. Boundaries in a polycrystalline material connect together at triple junctions. In this paper, we examine how the distribution of low angle boundaries at triple junctions varies with the texture of a material.

Thesis Advisor: Christopher Schuh

1 Introduction

Intergranular and transgranular phenomena in polycrystalline materials have been modeled by using percolation theory, treating the network of boundaries between different crystal grains as either strong or weak links. Different schemes to determine what constitutes a 'strong' link between grains have been proposed, such as low angle boundaries, CSL boundaries, or ability to transmit dislocations. Most models using standard percolation theory assume a random distribution of weak and strong links. However, it has been shown that the distribution of so called weak and strong boundaries is not necessarily random, and at triple junctions, where 3 boundaries come together, there are some constraints on the composition of the boundaries. The constraints at junctions change the distributions of triple junctions, which in turn changes how problems must be modeled using percolation theory.

There are four types of triple junctions that can occur in a material, as shown in Figure 1. These junctions have between zero and three low angle boundaries.
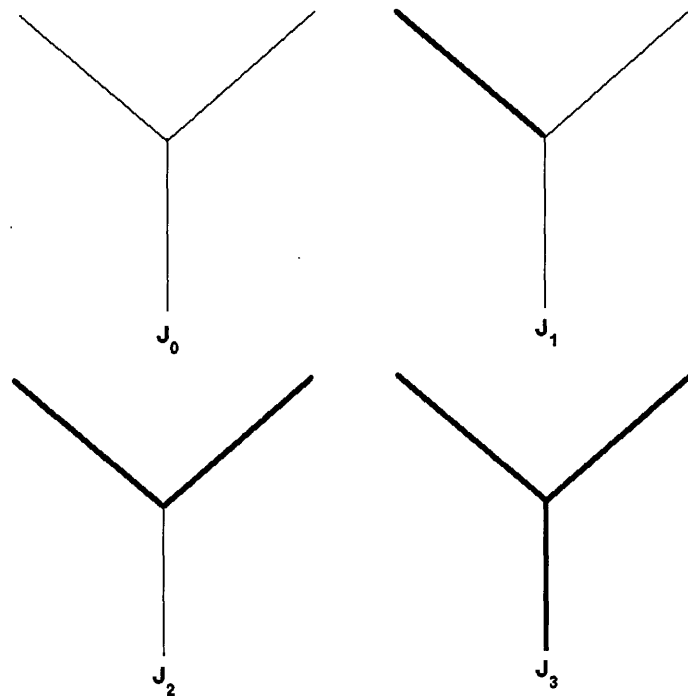

Figure 1. Types of triple junctions. Dark lines are 'strong' boundaries, light lines are 'weak' boundaries

The relative fractions of these junctions in the material can affect properties that percolate through the material along grain boundaries, as the triple junctions are the basic unit that connects grain boundaries together.

Grain boundaries with low misorientation angles are one type of boundary which are sometimes considered a 'strong' boundary. Low angle boundaries are sometimes thought to resist cracking or corrosion in materials. The distribution of orientations of the grains of a material, known as the texture, has been shown to influence the probabilities of types of boundaries that can occur in a material, and the distribution of the triple junctions [1]. In this paper, a method to solve for the distribution of triple junctions based off of two textures will be

2

developed. The first texture will be for a fiber texture, where orientations are defined by rotating about one axis from a reference orientation. In this paper, the distribution of triple junctions has been solved for this case using a different method. The second texture examined will be for a general texture, in which grains can have arbitrary orientations in three dimensions.

2 Local Transition Probabilities

In solving for the fiber texture, Frary et al. defined something called local transition probabilities to solve for the triple junctions [1]. These probabilities were defined as Π_x^y, the probability of examining a boundary in a triple junction that has not yet been examined, and finding a low angle boundary after examining y boundaries in the triple junction and having had x of them be low angle boundaries.

To determine the probability of having a low angle grain boundary depending on which boundaries of the junctions have already been examined, the problem is set up examining the boundaries one at a time. First, look at the boundary between grain A and grain B, and determine if it is a high angle or low angle boundary. Next, look at the boundary between grains B and C, and then finally between A and C. The possibilities for high or low angle boundaries are given in table

	J_0	$J_1/3$	$J_1/3$	$J_1/3$	$J_2/3$	$J_2/3$	$J_2/3$	J_3
AB	H	H	H	L	H	L	L	L
BC	H	H	L	H	L	H	L	L
AC	H	L	H	H	L	L	H	L

Table 1. Different ways that high and low angle boundaries can be distributed at a triple junction

The first column in the table is the only way that the boundaries can be chosen to have a J_0 boundary (all high angle). The next three columns are the three ways that boundaries can be picked to form a J_1 boundary. Because the choice of what the grains were named and therefore which boundary was labeled AB, BC, or AC was arbitrary, these three columns have an equal probability of occurring. Their probabilities must sum to J_1, hence each column has a probability of $J_1 / 3$. Similarly, the next three columns occur with a probability of $J_2 / 3$, while the last column represents J_3.

The probability of picking one low angle boundary without having looked at any other boundaries can be seen from the first row of the table. Any column is initially possible, and to pick a low angle boundary we must be in column 4, 6, 7, or 8. The probabilities of these

columns added together gives the initial probability p of finding a low angle boundary in the material, or:

$$p = \Pi_0^0 = \frac{J_1}{3} + \frac{2J_2}{3} + J_3 \quad (2.1)$$

To find Π_1^1, we know we have looked at the first row and found a low angle boundary, so we are only looking in the space of columns 4, 6, 7, and 8. Out of these columns, only 7 and 8 have a low angle boundary for the second boundary. Pi11 is equal to the probability of finding a low angle boundary given that you already have found one boundary, or in other words the probability of being in column 7 or 8 divided the probability that you were in column 4, 6, 7, or 8.

$$\Pi_1^1 = (\frac{J_2}{3} + J_3) / (\frac{J_1}{3} + \frac{2J_2}{3} + J_3) \quad (2.2)$$

Π_0^1 is columns 3 and 5 divided by columns 1, 2, 3, and 5.

$$\Pi_0^1 = (\frac{J_2}{3} + \frac{J_1}{3}) / (\frac{J_2}{3} + \frac{2J_1}{3} + J_0) \quad (2.3)$$

Π_2^2 is column 8 divided by columns 7 and 8.

$$\Pi_2^2 = J_3 / (\frac{J_2}{3} + J_3) \quad (2.4)$$

Π_1^2 is columns 5 and 6 divided by columns 3, 4, 5, and 6.

$$\Pi_1^2 = (\frac{2J_2}{3}) / (\frac{2J_2}{3} + \frac{2J_1}{3}) \quad (2.5)$$

And finally, Π_0^2 is column 2 divided by columns 1 and 2.

$$\Pi_0^2 = (\frac{J_1}{3}) / (J_0 + \frac{J_1}{3}) \quad (2.6)$$

These transition probabilities set up a system of equations for the junction probabilities. In combination with the fact that the junction probabilities need to add up to 1,

$$J_0 + J_1 + J_2 + J_3 = 1 \quad (2.7)$$

only three of the transition probabilities would need to be solved in order to determine the junction probabilities.

3 The effect of texture on triple junction distributions

Two types of textures are examined here, a fiber texture and a general texture. In both cases, we define the texture by picking some reference orientation, and letting grains take a random orientation by rotating up to some amount ϕ_{max}. In the case of the fiber texture, grains are only allowed to rotate about one axis away from the reference orientation, while for the general texture, grains are allowed to rotate about any axis. For each case, a boundary is called a low angle boundary if the misorientation angle between the two grains forming the boundary is less than some low angle boundary limit, θ_{LAB}.

3.1 Fiber texture

The first step to find the junction probabilities for the case of fiber texture is to solve for

4

the probability of a low angle boundary between any two grains, p. In order to accomplish this, the construction shown in Figure 2 is examined.
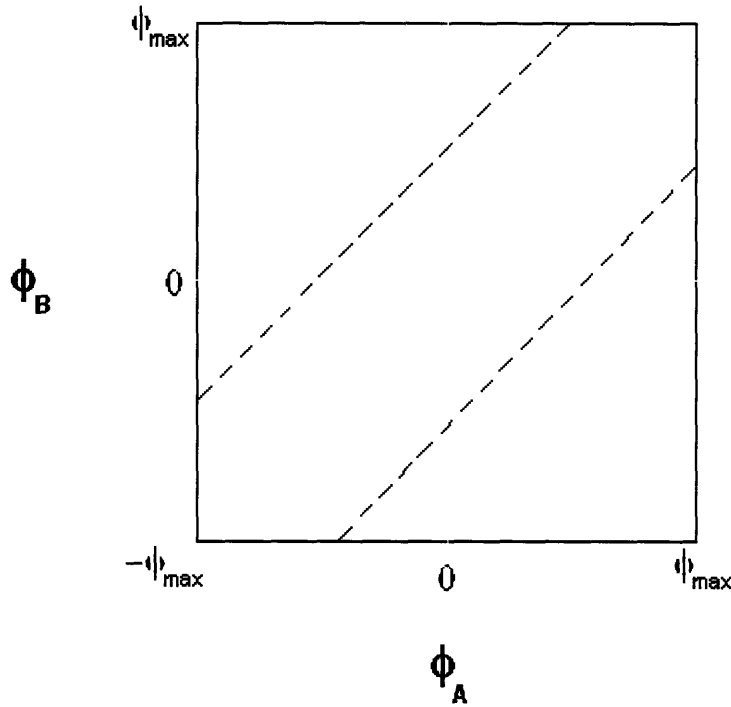

Figure 2. A representation of orientations for pairs of grains in fiber texture. The area inside of the dashed lines contains the points for which the grains share a low angle boundary.

The horizontal axis represents the angle that grain A was rotated from the reference orientation, while the vertical axis represents the angle for grain B. Each point of the diagram then represents a pair of orientations for grain A and B. As the orientations of the grains are independent and randomly chosen, all points within the diagram are equally likely, so long as the angles for A and B are between $-\phi_{max}$ and ϕ_{max}. In this diagram, the area contained between the two dashed lines represents the orientations for grains A and B which are within θ_{LAB} of one another, and therefore cause the AB boundary to become a low angle boundary. Because all of the points in this space are equally probable, the probability of a low angle boundary is simply the area of the area inside of the dashed lines divided by the total area of the space. This comes out to be[1]

$$p = \frac{\theta_{LAB}}{\phi_{max}} - \frac{\theta_{LAB}^{2}}{4\phi_{max}^{2}} \qquad (3.1)$$

Note that this equation can be expressed in terms of the ratio $\theta_{LAB} / \phi_{max}$. This can be seen in figure 1, as the figure would look the same if all of the angles in the figure were doubled. If the ratio is explicitly defined as

---

[1] See appendix A for derivation

5

$$X = \frac{\theta_{LAB}}{\phi_{max}}$$

(3.2)

then the equation for p becomes

$$p = X - \frac{X^2}{4}$$

(3.3)

The next step of the analysis involves adding grain C into the picture, as shown in figure 3.
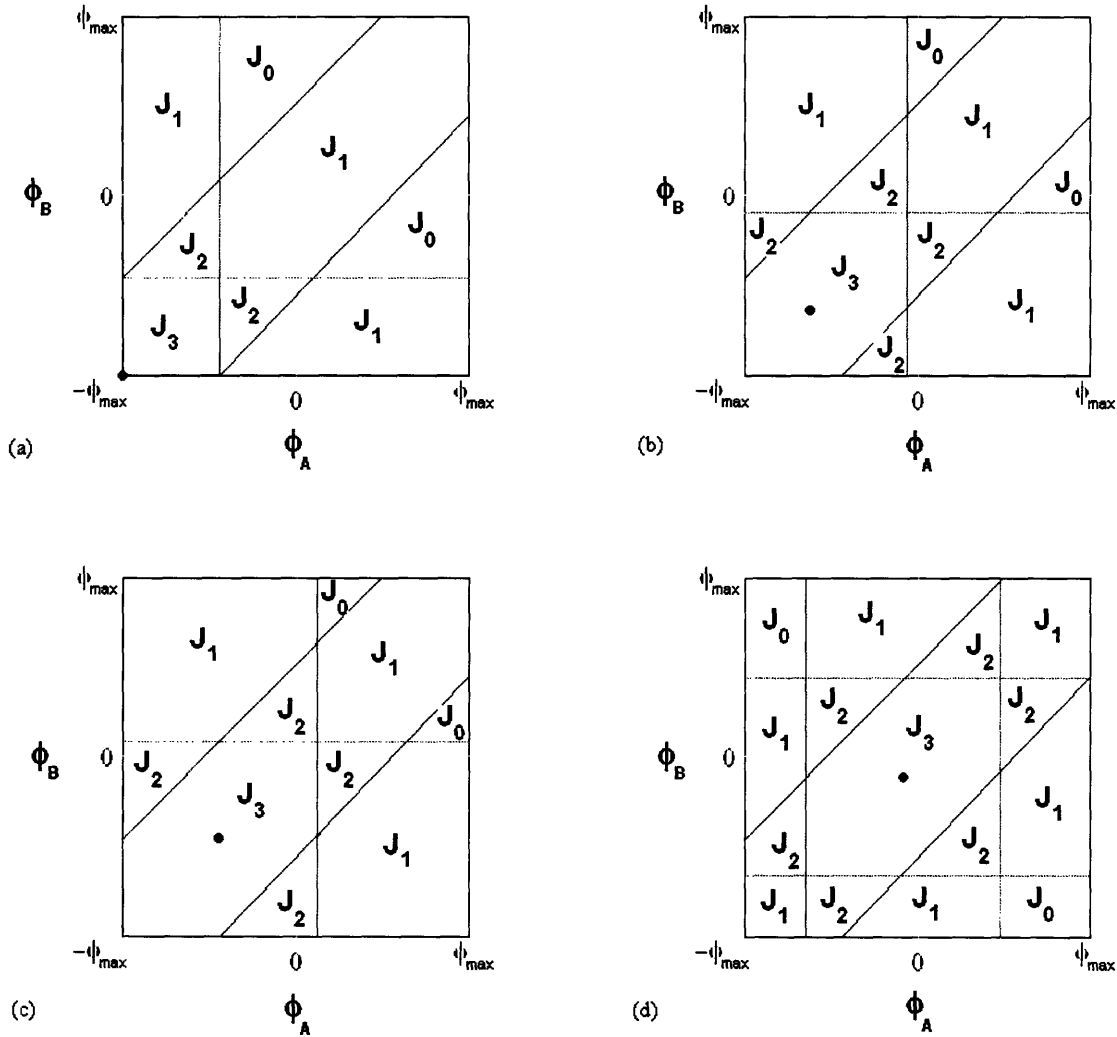

Figure 3. A representation of orientations for grains A and B for specific orientations of C. The position of the black dot projected on either axis gives the orientation of grain C.

In part (a) of the figure, grain C is at an orientation rotated $-\phi_{max}$ from the reference orientation. As before, the region in space between the two diagonal lines is the region where the AB boundary is a low angle boundary. With the addition of the grain C, the region below the horizontal line indicates the points where the AC boundary is low angle, and the region to the left of the vertical line indicates a low angle BC boundary. The lines then break up the space into the

6

various types of junctions, which are labeled on the diagram. Grain C is then let move from it's orientation of $-\phi_{max}$ up to the reference orientation in parts (b) to (d). By integrating the areas of the various regions as grain C moves, volumes proportional to the probabilities of the various junctions can be found[2], similar to how the area proportional to p was found above. The probabilities for the various types of junctions are found to be:

$$J_0 = 1 - 3X + 3X^2 - X^3 \qquad\qquad X<1 \qquad (3.4a)$$

$$J_0 = 0 \qquad\qquad X>1 \qquad (3.4b)$$

$$J_1 = 3X - \frac{9X^2}{2} + \frac{7X^3}{4} \qquad\qquad X<1 \qquad (3.5a)$$

$$J_1 = 2 - 3X + \frac{3X^2}{2} - \frac{X^3}{4} \qquad\qquad X>1 \qquad (3.5b)$$

$$J_2 = \frac{3X^2}{4} - \frac{X^3}{2} \qquad\qquad X<1 \qquad (3.6a)$$

$$J_2 = -1 + 3X - \frac{9X^2}{4} + \frac{X^3}{2} \qquad\qquad X>1 \qquad (3.6b)$$

$$J_3 = \frac{3X^2}{4} - \frac{X^3}{4} \qquad\qquad (3.7)$$

3.2 General texture

To determine the junction probabilities for general texture, a way to represent arbitrary orientations in space must be chosen. For this derivation, quaternions are used to represent orientation. Quaternions can be thought of as points on the surface of a four dimensional unit sphere. A coordinate system can be defined for the sphere with the axes x, y, z, and w. Points on the sphere can then be defined by a vector (x,y,z,w). Orientations are defined from a reference orientation at (0,0,0,1). A rotation from the reference orientation of an angle theta about an axis (x,y,z) is represented on the sphere by rotating away from the reference orientation by an angle of theta/2, in the direction of (x,y,z,0). Misorientation angles between two grains in this space are represented half of the angular distance between their orientations on the surface of the quaternion sphere. The density of grain orientations is uniform over the surface of this sphere.[3]

If ϕ_{max}, the maximum angle from a reference orientation that we allow grains to rotate to, is less than approximately 40 degrees, then the angle covered on the surface of the hypersphere will be less than 20 degrees. If the only orientations that are considered are orientations that are within ϕ_{max} of the reference orientation, a low angle approximation can then be used, where the surface of the hypersphere can then be projected onto a solid three dimensional sphere, much like the surface of a 3 dimensional sphere can be projected onto a solid 3 dimensional disk. Uniform density of grain orientations is preserved in the low angle approximation. Orientations are now represented by points within a solid 3 dimensional sphere, of radius $\phi_{max}/2$ (with angles in radians). The distance between two points divided by two represents the misorientation angle of two grains with orientations defined by those points. This means that each point representing an orientation has a sphere around it of radius $\theta_{LAB}/2$, and all points lying within this sphere

---

[2] See appendix B for details
[3] See appendix C for derivation

7

represent orientations which would share a low angle boundary with the orientation at the center of the sphere. At this point, the space can be scaled by a factor of 2, so orientations are represented within a sphere of radius ϕ_{max}, and misorientation angles are simply the distance between two points.

Figure 4 shows a plane section of the spherical orientation space, with the reference orientation at the center of the large circle. The large circle is the section of the sphere within which are orientations existing in the texture. An orientation for grain A is shown, around which there is a smaller circle. Points within the smaller circle represent orientations for which grains would share a low angle boundary with grain A.
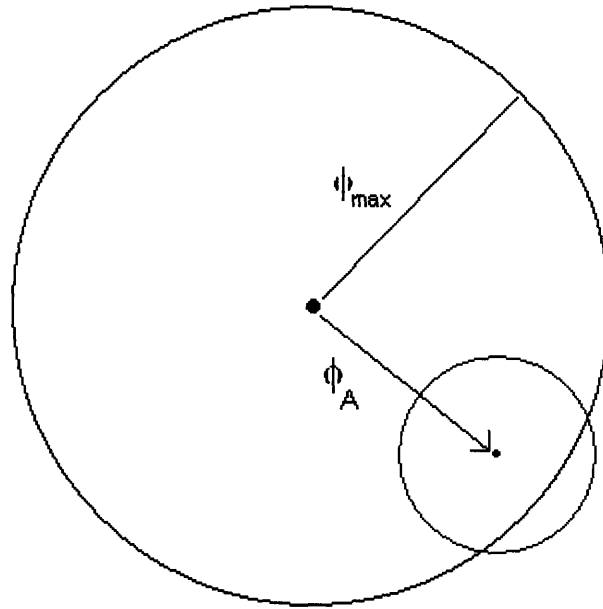

Figure 4. A section of the spherical space of possible orientations a grain can take. Grain A is rotated by some angle away from the reference orientation, and an points near it represent orientations which would form low angle boundaries with grain A

If the orientation of grain B was picked randomly within ϕ_{max} of the reference orientation, it could fall anywhere within the sphere centered at the reference orientation. The AB boundary would be low angle if grain B fell within the sphere centered at the orientation of grain A. Because the density of orientations is even throughout the space, the probability of a low angle boundary for this particular orientation of grain A proportional to the volume of space that grain B could fall in which is inside the sphere centered at grain A, that is, the intersection volume of the two spheres. By integrating this volume as grain A moves over the orientations that it is allowed to take on, the probability p of a low angle boundary for a material of this texture can be found.[4]

$$p = X^3 - \frac{18X^2}{32} + \frac{X^3}{32}$$

(3.8)

Figure 5 shows some possibilities for fixing the orientations of grains A and B, and

---

[4] See appendix D for details
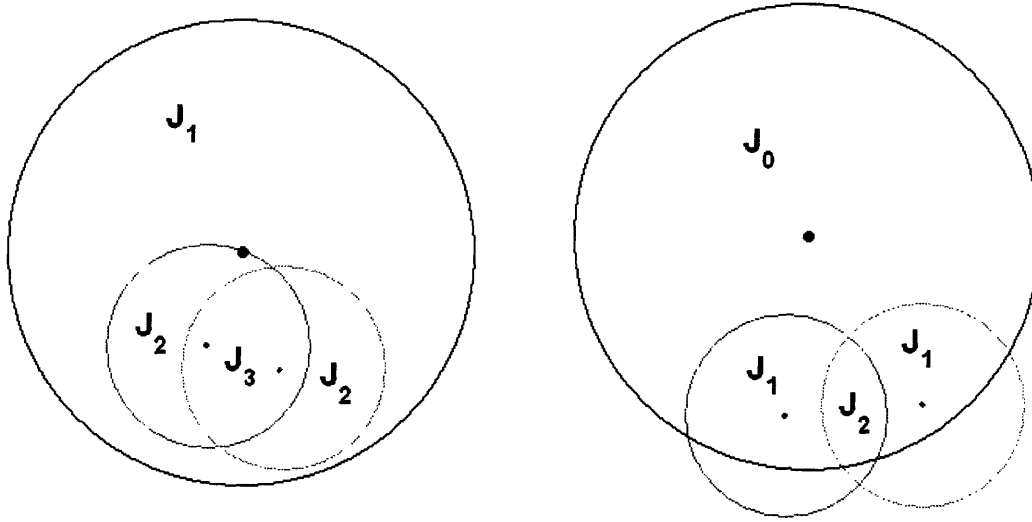
8

letting grain C fall anywhere in the space.

Figure 5. A section of the sphere that represents the orientation space for general texture, with possible orientations of two grains shown inside the sphere. The types of junctions that would result from a third grain having an orientation within a certain area are labeled.

By integrating the volumes as grains A and B move over the space, the various junction probabilities can be found. Unfortunately these integrals are somewhat difficult to set up, and integrals for the volumes have not been completed at this time. However, integrals leading to another constraint on the system have been completed. It is possible to find the volume for which the AB and BC boundaries are low angle boundaries. Looking at table 1, this corresponds to $J_3 + J_2/3$.[5]

$$J_3 + \frac{J_2}{3} = \frac{2120X^9 + 2835X^8 - 25488X^7 + 26880X^6}{26880} \qquad X<1 \quad (3.9a)$$

$$J_3 + \frac{J_2}{3} = \frac{-440X^9 + 2835X^8 - 4752X^7 + 26880X^6 - 20736X^5 + 2560}{26880} \qquad X>1 \quad (3.9b)$$

Combining equation (3.9) with equations (2.1), (3.8), and (2.7) gives us three constraints on the distribution of J_0, J_1, J_2, and J_3. This means that solving for any one of the junction probabilities will give us the other three. The largest misorientations that three grains can have in this space are when they are spaced in an equilateral triangle, with each grain rotated ϕ_{max} from the reference orientation. When the grains are at these locations, they are at the corners of a triangle inscribed in a circle of radius ϕ_{max}. The distance between the grains is then sqrt(3) * ϕ_{max} apart from each other. Hence, for θ_{LAB} greater than sqrt(3) * ϕ_{max}, there must be at least one low angle boundary in a triple junction, and J_0 is therefore equal to zero. Using the above constraints, we can solve for the other triple junctions.

$$J_3 = \frac{9}{7} - \frac{81X^2}{35} + \frac{27X^4}{16} - \frac{3X^6}{32} - \frac{297X^7}{560} + \frac{81X^8}{256} - \frac{11X^9}{224} \qquad (3.10)$$

---

[5] See Appendix E for details

$$J_2 = -\frac{25}{7} + \frac{162X^2}{35} + 3X^3 - \frac{81X^4}{16} + \frac{9X^6}{32} + \frac{297X^7}{280} - \frac{81X^8}{128} - \frac{11X^9}{112} \qquad (3.11)$$

$$J_1 = \frac{23}{7} - \frac{81X^2}{35} - 3X^3 + \frac{27X^4}{8} - \frac{3X^6}{16} - \frac{297X^7}{560} + \frac{81X^8}{256} - \frac{11X^9}{224} \qquad (3.12)$$

$$J_0 = 0 \qquad (3.13)$$

However, the solution for X less than the square root of three still requires the solution of one of the probabilities for one of the junctions.

4. Results and discussion

The geometric methods presented here seem to provide a way to find analytical solutions to the distribution of triple junctions for various textures. These methods could be applied to non-uniform textures if a weighting function was applied to the integrals.

For the constraints found for the general texture, the integrals had to be broken up into multiple parts, and yet the answers were sometimes continuous across those parts. As we have full solutions for the general texture for X greater than the square root of three, it seems tempting to attempt to assume that one of the junctions has the same solution for X less than the square root of three. However, because the constraints in equations (2.7), (3.8), and (3.9b) are all continuous at X equal to the square root of three, if any one of the functions for the junction probabilities is continuous, all of the junction probabilities would be continuous. However, it is evident that J_0 is not continuous, so all of the junctions must have a discontinuity in their functions at X equal to the square root of three.

Appendix A
Derivation of probability of a low angle boundary for fiber texture

As discussed in section 3.1, the area AreaP inside of the dotted lines in Figure 1 is proportional to the probability of having a low angle boundary in a fiber textured material. In order to find the area in that figure, we use the construction shown in Figure A1.
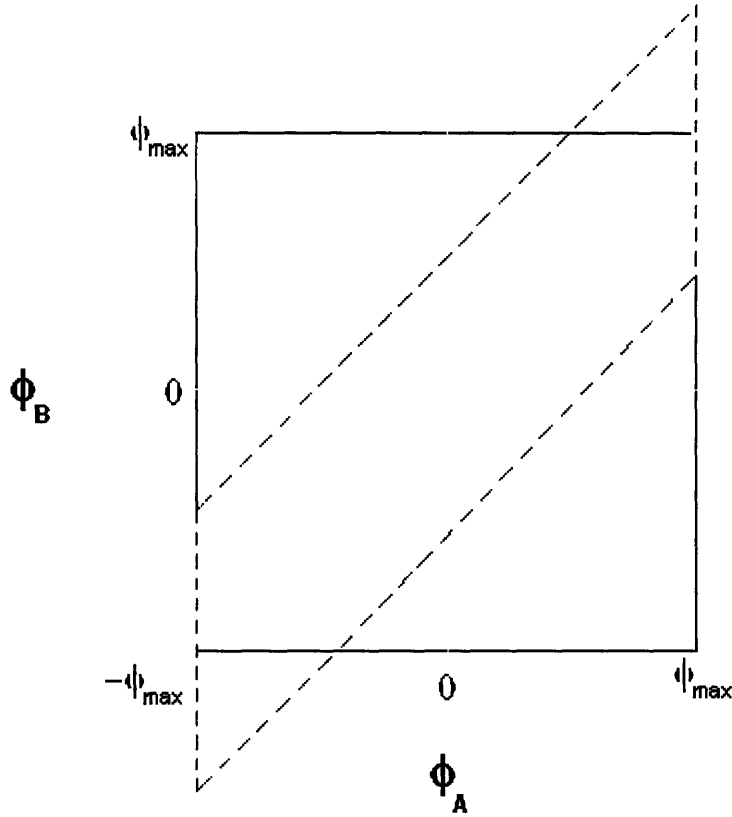
Figure A 1. The same figure as figure 2, with an additional geometric construction to enable the solution of the area for low angle boundaries

The area of the parallelogram minus the area of the two triangles contained in the parallelogram is the area that we are trying to find. The area of the parallelogram can be found by integrating the height of the parallelogram over ϕ_A from $-\phi_{max}$ to ϕ_{max}. As the height is a constant 2 times θ_{LAB}, the area comes out to be $4 * \phi_{max} * \theta_{LAB}$. Each of the triangles is a right triangle with legs of length θ_{LAB}. The area of each triangle is then $\theta_{LAB}^2 / 2$. Subtracting the area of the two triangles from the area of the parallelogram, we get

$$AreaP = 4\phi_{max}\theta_{LAB} - 2\frac{\theta_{LAB}^2}{2} \tag{A.1}$$

To find P, we then divide the area found by the total area of the space of the allowed grain orientations. The space of the allowed grain orientations is a square that is $2 * \phi_{max}$ on a side, so the area is $4 * \phi_{max}^2$. This gives us

$$p = \frac{\theta_{LAB}}{\phi_{max}} - \frac{\theta_{LAB}^2}{4\phi_{max}^2} \tag{A.2}$$

Appendix B

11

Derivation of junction probabilities for fiber texture

There are two regimes of X to be concerned with for deriving the probabilities of different types of fiber texture triple junctions, the first where θ_{LAB} is between zero and ϕ_{max}, and the second where θ_{LAB} is between ϕ_{max} and $2 * \phi_{max}$. In either case, only two of the junction probabilities need to be solved for, as the constraints in equations (2.1) and (2.7) will allow the other two to be solved for.

In the first regime, where θ_{LAB} is less than ϕ_{max}, Figure 1 may be used to find the volumes of the regions. First, to find J_3, (a) to (c) of Figure 3 is examined to determine what happens as the orientation of C moves from $-\phi_{max}$ to $-\phi_{max} + \theta_{LAB}$. It can be seen that in part (a), J_3 covers an area of θ_{LAB}^2. J_3 then linearly increases as the orientation of C increases, until grain C reaches a orientation of $-\phi_{max} + \theta_{LAB}$. At this point, the J_3 has an area of $3\theta_{LAB}^2$, as can be seen from Figure B1.
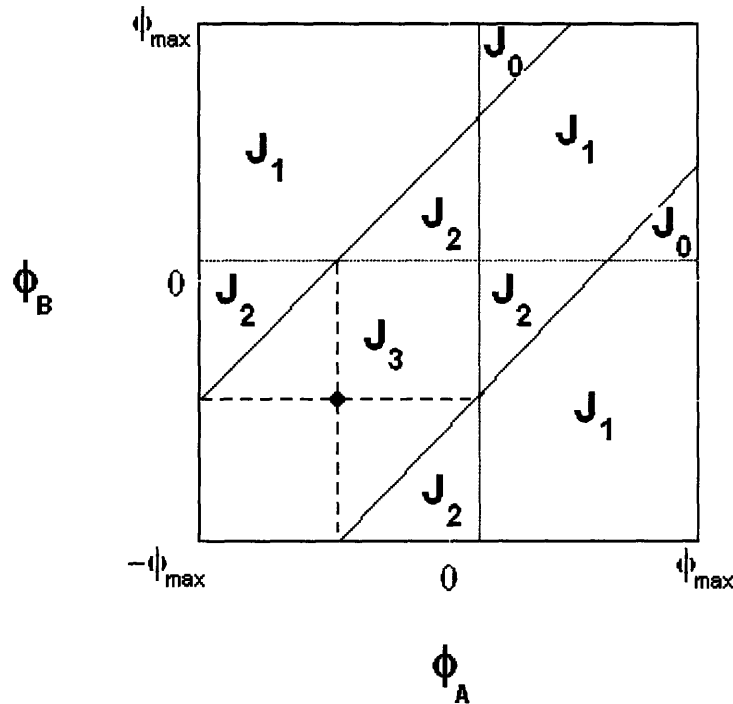

Figure B 1. An expanded version of Figure 3c, with lines drawn in to find the area of J_3

The average area of J_3 in this region is then $2\theta_{LAB}^2$. The volume this sweeps out is equal to the average area multiplied by the distance that grain C travels, θ_{LAB}. The volume in this region is therefore $2 * \theta_{LAB}^3$. The second region to examine is where the orientation of C is between $-\phi_{max} + \theta_{LAB}$ and 0. In this region, the area of J_3 is constant at $3* \theta_{LAB}^2$. The volume swept out is then $3* \theta_{LAB} *(\phi_{max} - \theta_{LAB})$. for orientations of C greater than zero, the diagrams are symmetric to the ones for orientations less than zero, and the volume swept out can simply be doubled to account for those orientations of C. Therefore

$$VolumeJ_3 = 2(2\theta_{LAB}^3 + 3\theta_{LAB}(\phi_{max} - \theta_{LAB})) \qquad (B.1)$$

The probability of a J_3 junction is the volume of this J_3 region, divided by the volume of the space of possible orientations. The total possible volume of the space is the volume of the square that makes up the orientations for A and B, $(2* \phi_{max})^2$, times the distance that the possible orientations of C can take, $2* \phi_{max}$. The total volume of the space of allowed orientations is

$$VolumeSpace = 8\phi_{max}{}^3 \qquad (B.2)$$

which makes the probability of a J_3 junction

$$J_3 = \frac{VolumeJ_3}{VolumeSpace} = \frac{3X^2}{4} - \frac{X^3}{4} \qquad (B.3)$$

To find J_2 in the first regime, the area where the AB boundary is a high angle boundary, but the BC and AC boundaries are low angle is examined. From table 1, the area of this region is $J_2/3$. While the orientation of C increases between $- \phi_{max}$ and $- \phi_{max} + \theta_{LAB}$, this area is made up of two right triangles whose side lengths increase linearly with C, up to a side length of θ_{LAB}. The volume swept out is that of two pyramids, with a base areas of $\theta_{LAB}{}^2/2$, and a height of the distance C moved, θ_{LAB}. The volume of the each pyramids is then $\theta_{LAB}{}^3/6$. While the orientation of C moves between $- \phi_{max} + \theta_{LAB}$ and 0, the area of this region is constant, made of two right triangles of side length θ_{LAB}, and area $\theta_{LAB}{}^2/2$. The total volume is therefore

$$\frac{VolumeJ_2}{3} = 2(\frac{\theta_{LAB}{}^3}{6} + \theta_{LAB}{}^2(\phi_{max} - \theta_{LAB})) \qquad (B.4)$$

$$J_2 = \frac{VolumeJ_2}{VolumeSpace} \qquad (B.5)$$

combining equations (B.5) and (B.2),

$$J_2 = \frac{3X^2}{4} - \frac{X^3}{2} \qquad (B.6)$$

Using equations (2.1), (2.7), (3.3), (B.3),and (B.6), J_1 and J_0 can be found to be

$$J_0 = 1 - 3X + 3X^2 - X^3 \qquad (B.7)$$

$$J_1 = 3X - \frac{9X^2}{2} + \frac{7X^3}{4} \qquad (B.8)$$

for ϕ_{max} greater than θ_{LAB}.

For the second regime, where θ_{LAB} is greater than ϕ_{max}, Figure B2 is used. It can be noted that J_0 is equal to zero for this regime.
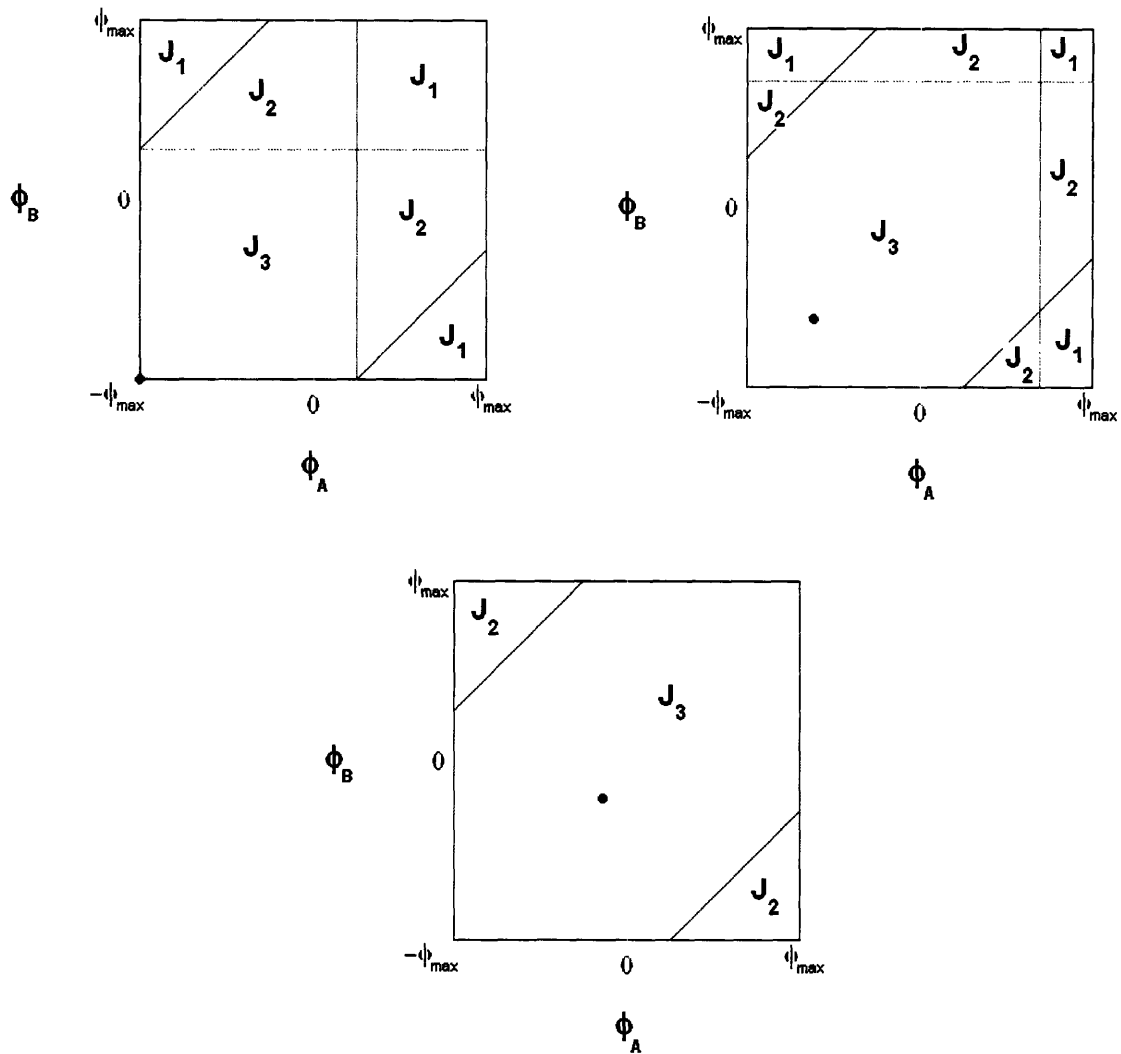
Figure B 2. A representation for possible orientations of grains for fiber texture when ϕ_{max} is less than θ_{LAB}

Here, the region for $J_1/3$ where the AB boundary is low angle is examined. As grain C moves between $-\phi_{max}$ and ϕ_{max} -theta, a square pyramid is swept out, with a base of $(2 \phi_{max} - \theta_{LAB})^2$ and a height of $2 \phi_{max} - \theta_{LAB}$. This gives

$$\frac{VolumeJ_1}{3} = \frac{2(\phi_{max} - \theta_{LAB})^3}{3} \tag{B.9}$$

$$J_1 = \frac{VolumeJ_1}{VolumeSpace} \tag{B.10}$$

$$J_1 = 2 - 3X + \frac{3X^2}{2} - \frac{X^3}{4} \tag{B.11}$$

Combining this with

$$J_0 = 0$$

14

and equations (2.1), (A.2) and (2.7) gives

$$J_2 = -1 + 3X - \frac{9X^2}{4} + \frac{X^3}{2}$$

$$J_3 = \frac{3X^2}{4} - \frac{X^3}{4}$$

Appendix C
Demonstration of even coverage of points for quaternions

For a given rotation of angle d from the reference orientation on a quaternion sphere, the density of points for random orientations on a quaternion is proportional to $\sin^2(d/2)$. [2] Translating to rotations on the unit hypersphere, the density of points is proportional to $\sin^2(\theta)$, where θ is the angle of rotation on the hypersphere. If the four dimensional space is sectioned at a constant value of w, a three dimensional space with a spherical shell of radius $\sin(\theta)$ results. The area of this shell is proportional to $\sin^2(\theta)$, and hence the density of points is constant for a given area.

Appendix D
Constraints on general texture

To solve for p for general texture, a method similar to the solution shown in Appendix A for fiber texture can be used. The volume swept out by the sphere that determines a low angle boundary for grain A is taken as the orientation of A changes, and the amount of the sphere that is outside of the space of allowed orientations is subtracted off from that. The volume swept out by the sphere as grain A moves in the orientation space is simply the size of the space, $4\pi/3$ * ϕ_{max}^3, times the size of the sphere about grain A, $4\pi/3$ * θ_{LAB}^3. To find the amount of the sphere outside the space of allowed orientations, the construction in Figure D1 is used.
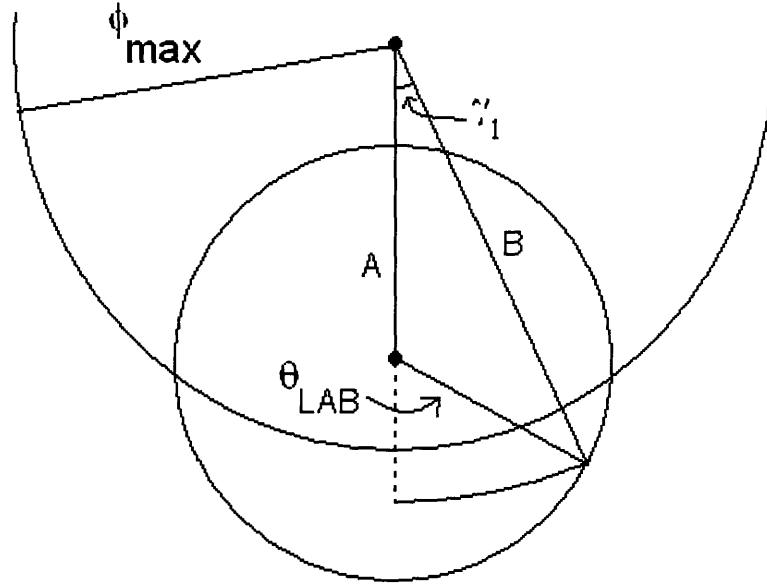
Figure D 1. A construction to solve for the volume of space that represents orientations that would share a low angle boundary with grain A, but are outside the allowed space for the texture.

Grain A must be within θ_{LAB} of the boundary of the allowed orientations for part of the sphere to be outside, so the integral for A goes from $\phi_{max} - \theta_{LAB}$ to ϕ_{max}. The integral is weighted by the area for which grain A could be that distance from the boundary, the area of a spherical shell of radius A, $4\pi A^2$. B is then integrated over the outside area in spherical caps of an angle γ_1, centered at the reference orientation. A spherical cap of angle gamma on a sphere of radius R has an area Ar given by

$$Ar = 2\pi R^2 (1 - Cos(\gamma_1)) \tag{D.1}$$

By the law of cosines,

$$Cos(\gamma_1) = \frac{A^2 + B^2 - \theta_{LAB}^2}{2AB} \tag{D.2}$$

The area outside the space Ao is then

$$Ao = \int_{\phi_{max}-\theta_{LAB}}^{\phi_{max}} dA * 4\pi A^2 \int_{\phi_{max}}^{A+\theta_{LAB}} dB * 2\pi B^2 (1 - Cos(\gamma_1)) \tag{D.3}$$

The area for p becomes

$$AreaP = \left(\frac{4\pi}{3}\right)^2 \phi_{max}^3 \theta_{LAB}^3 - Ao \tag{D.4}$$

Integrating for Ao and dividing AreaP by the volume of the allowed space for pairs of orientations for grains, $(4\pi\phi_{max}^3/3)^2$, this becomes

16

$$p = \frac{AreaP}{\left(\frac{4\pi\phi_{max}^{3}}{3}\right)^{2}} = X^3 - \frac{18X^2}{32} + \frac{X^3}{32} \qquad (D.5)$$

The above derivation only holds for θ_{LAB} less than ϕ_{max}. For θ_{LAB} greater than ϕ_{max}, a similar construction in Figure D2 is used. However, instead of integrating for p, here the integral is for q, the probability of a high angle boundary, where
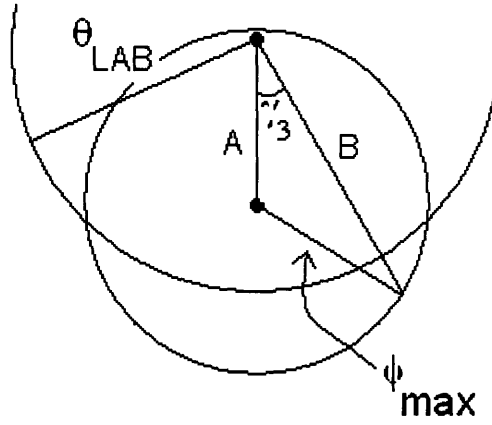
$$q = 1 - p \qquad (D.6)$$

Figure D 2. A construction to solve for the probability of a high angle boundary in the general texture

In this case the area can be found directly through integration. From the law of cosines,

$$Cos(\gamma_3) = \frac{A^2 + B^2 - \phi_{max}^{2}}{2AB} \qquad (D.7)$$

Integrating for the allowed space where grain B can fall to not cause a low angle boundary yields

$$AreaQ = \int_{\theta_{LAB}-\phi_{max}}^{\phi_{max}} dA * 4\pi A^2 \int_{\theta_{LAB}}^{A+\phi_{max}} dB * 2\pi B^2 (1 - Cos(\gamma_3)) \qquad (D.8)$$

$$q = \frac{AreaQ}{\left(\frac{4\pi\phi_{max}^{3}}{3}\right)^{2}} \qquad (D.9)$$

Solving through for p yields the same equation as in D.5, despite having a different derivation. This means that there is only one formula for p for the entire range of X.

Appendix E

To solve for $J_3 + J_2/3$, the integrals are set up as follows: Grain A can move over the entire space. Grain B can move anywhere within θ_{LAB} of grain A, and grain C can then move within θ_{LAB} of grain B. The problem must be broken up into many different regimes of X in

17

order to solve it. To simplify some of the integrals, the idea of integrating on the space outside the allowed orientations in the texture is used for grain C. For X less than 1, the following equation holds for the integral of the outside area for C, Aoc.

$$J_3 + \frac{J_2}{3} = pX^\wedge 3 - \frac{Aoc}{\left(\frac{4\pi\phi^3}{3}\right)^3}$$

(E.1)

To complete the integrals, the math coming from figure D1 can be used for grain B. A similar figure could be used to get from grain B to grain C, yielding

$$Cos(\gamma_2) = \frac{B^2 + C^2 - \theta_{LAB}^{\ \ 2}}{2BC}$$

(E.2)

For X less than 0.5, there are two integrals which must be added together, one where grain A is within θ_{LAB} of the boundary of the space, and one where it is within $2\theta_{LAB}$ of the boundary. Hence in this region,

$$Aoc = Aoc1 + Aoc2$$

(E.3)

$$Aoc1 = \int_{\phi_{max}-\theta_{LAB}}^{\phi_{max}} dA * 4\pi A^2 \int_{\phi_{max}-\theta_{LAB}}^{\phi_{max}} dB * 2\pi B^2 (1 - Cos(\gamma_1)) \int_{\phi_{max}}^{B+\theta_{LAB}} dC * 2\pi C^2 (1 - Cos(\gamma_2))$$

(E.4)

$$Aoc2 = \int_{\phi_{max}-2\theta_{LAB}}^{\phi_{max}-\theta_{LAB}} dA * 4\pi A^2 \int_{\phi_{max}-\theta_{LAB}}^{A+\theta_{LAB}} dB * 2\pi B^2 (1 - Cos(\gamma_1)) \int_{\phi_{max}}^{B+\theta_{LAB}} dC * 2\pi C^2 (1 - Cos(\gamma_2))$$

(E.5)

Combining equations (E.1), (E.3), (E.4), and (E.5) yields

$$J_3 + \frac{J_2}{3} = \frac{2120X^9 + 2835X^8 - 25488X^7 + 26880X^6}{26880}$$

(E.6)

For X between one half and two thirds, the following equations are used to find Aoc:

$$Aoc = Aoc3 + Aoc4 + Aoc5 + Aoc6$$

(E.7)

$$Aoc3 = \int_{\phi_{max}-\theta_{LAB}}^{\phi_{max}} dA * 4\pi A^2 \int_{\phi_{max}-\theta_{LAB}}^{\phi_{max}} dB * 2\pi B^2 (1 - Cos(\gamma_1)) \int_{\phi_{max}}^{B+\theta_{LAB}} dC * 2\pi C^2 (1 - Cos(\gamma_2))$$

(E.8)

$$Aoc4 = \int_{2\theta_{LAB}-\phi_{max}}^{\phi_{max}-\theta_{LAB}} dA * 4\pi A^2 \int_{\phi_{max}-\theta_{LAB}}^{A+\theta_{LAB}} dB * 2\pi B^2 (1 - Cos(\gamma_1)) \int_{\phi_{max}}^{B+\theta_{LAB}} dC * 2\pi C^2 (1 - Cos(\gamma_2))$$

(E.9)

$$Aoc5 = \int_{0}^{2\theta_{LAB}-\phi_{max}} dA * 4\pi A^2 \int_{\theta_{LAB}-A}^{A+\theta_{LAB}} dB * 2\pi B^2 (1 - Cos(\gamma_1)) \int_{\phi_{max}}^{B+\theta_{LAB}} dC * 2\pi C^2 (1 - Cos(\gamma_2))$$

(E.10)

$$Aoc6 = \int_{0}^{2\theta_{LAB}-\phi_{max}} dA * 4\pi A^2 \int_{\phi_{max}-\theta_{LAB}}^{\theta_{LAB}-A} dB * 4\pi B^2 \int_{\phi_{max}}^{B+\theta_{LAB}} dC * 2\pi C^2 (1 - Cos(\gamma_2))$$

(E.11)

Solving the equations results in equation (E.6) again for this region.

For X between two thirds and one, again slightly different equations are used to find Aoc:

$$Aoc = Aoc7 + Aoc8 + Aoc9 + Aoc10$$

(E.12)

$$Aoc7 = \int_{2\theta_{LAB}-\phi_{max}}^{\phi_{max}} dA * 4\pi A^2 \int_{\phi_{max}-\theta_{LAB}}^{\phi_{max}} dB * 2\pi B^2 (1 - Cos(\gamma_1)) \int_{\phi_{max}}^{B+\theta_{LAB}} dC * 2\pi C^2 (1 - Cos(\gamma_2))$$

(E.13)

$$Aoc8 = \int_{\phi_{max}-\theta_{LAB}}^{2\theta_{LAB}-\phi_{max}} dA * 4\pi A^2 \int_{\theta_{LAB}-A}^{\phi_{max}} dB * 2\pi B^2 (1 - Cos(\gamma_1)) \int_{\phi_{max}}^{B+\theta_{LAB}} dC * 2\pi C^2 (1 - Cos(\gamma_2))$$

(E.14)

$$Aoc9 = \int_{0}^{\phi_{max}-\theta_{LAB}} dA * 4\pi A^2 \int_{\theta_{LAB}-A}^{\theta_{LAB}+A} dB * 2\pi B^2 (1 - Cos(\gamma_1)) \int_{\phi_{max}}^{B+\theta_{LAB}} dC * 2\pi C^2 (1 - Cos(\gamma_2))$$

(E.15)

$$Aoc10 = \int_{0}^{2\theta_{LAB}-\phi_{max}} dA * 4\pi A^2 \int_{\phi_{max}-\theta_{LAB}}^{\theta_{LAB}-A} dB * 4\pi B^2 \int_{\phi_{max}}^{B+\theta_{LAB}} dC * 2\pi C^2 (1 - Cos(\gamma_2))$$

(E.16)

In this region, $J_3 + J_2/3$ again comes out as in equation (E.6)

   As for finding p, when X becomes larger than one, it becomes easier to find high angle boundaries. Integration can be done to find where the AB and BC boundaries are both high angle. Looking at Table 1, this is $J_0 + J_1/3$. Note that from equations (2.1) and (2.7),

$$J_3 + \frac{J_2}{3} = 2p - 1 - (J_0 + \frac{J_1}{3})$$

(E.17)

Figure E1 shows the construction necessary to carry out the integral for $J_0 + J_1/3$

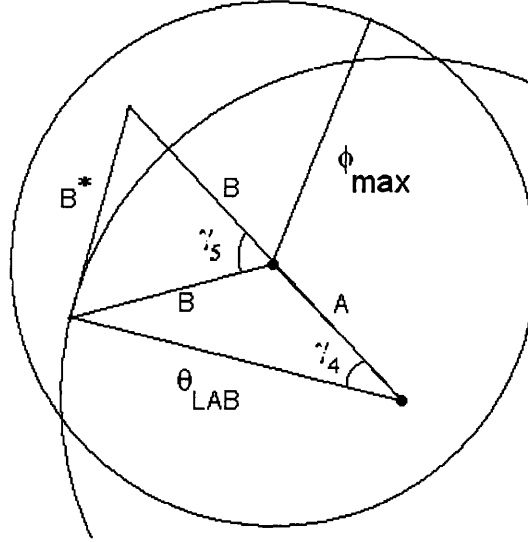**Figure E 1. Construction to find J0 + J1/3. This is slightly more complex than preceding constructions due to the need to change the point about which concentric spherical caps are being integrated from the orientation of grain A to the orientation of grain B.**

Using the law of cosines:

$$Cos\ (\gamma_4) = \frac{A^2 + \theta_{LAB}{}^2 - B^2}{2 A \theta_{LAB}}$$

(E.18)

$$Cos(\gamma_4) = \frac{(A+B)^2 + \theta_{LAB}{}^2 - (B^*)^2}{2(A+B)\theta_{LAB}}$$

(E.19)

$$Cos(\gamma_5) = \frac{2B^2 - (B^*)^2}{2B^2}$$

(E.20)

Combining (E.18) and (E.19),

$$(B^*)^2 = (A+B)^2 + \theta_{LAB}{}^2 - (A+B)(\frac{A^2 + \theta_{LAB}{}^2 - B^2}{2A})$$

(E.21)

The integral to find the area Ah for $J_0 + J_1/3$ is

$$Ah = \int_{\theta_{LAB}-\phi_{max}}^{\phi_{max}} dA * 4\pi A^2 \int_{\theta_{LAB}-A}^{\phi_{max}} dB * 2\pi B^2 (1 - Cos(\gamma_5)) \int_{\theta_{LAB}}^{B+\phi_{max}} dC * 2\pi C^2 (1 - Cos(\gamma_6))$$

(E.22)

where

19

$$Cos(\gamma_6) = \frac{C^2 + B^2 - \phi_{max}^{\ \ 2}}{2CB} \tag{E.23}$$

finally,

$$J_0 + \frac{J_1}{3} = \frac{Ah}{\left(\dfrac{4\pi\phi^3}{3}\right)^3} \tag{E.24}$$

Solving the integral and combining equations (E.24) with (E.17) and (D.5) yields

$$J_3 + \frac{J_2}{3} = \frac{-440X^9 + 2835X^8 - 4752X^7 + 26880X^6 - 20736X^5 + 2560}{26880} \tag{E.25}$$

Bibliography

[1] M. Frary and C. A. Schuh, Phys. Rev. B **69**, 134115 (2004)
[2] D. C. Handscomb, Can. J. Math., **10**, 85-87, (1958)